Search for Contact Interactions at $\sqrt{s} = 8$ TeV with the CMS Detector

Roberto Prado-Rivera
Department of Physics, Florida State University, Tallahassee, Florida

Abstract
We describe the search for evidence of new high energy interactions that can be modelled as contact interactions at the Large Hadron Collider. This search was done using the 8 TeV proton-proton collision data set from the Central Muon Solenoid detector at the LHC. We interpret the results in terms of a lower limit on the mass scale Λ of the left-left contact interaction model with constructive and destructive interference. The data was found to be consistent with the QCD prediction. The lower limit for constructive interference was found to be $\Lambda > 22.7$ TeV and for destructive interference was $\Lambda > 13.9$ TeV at 95% confidence level.

1 Introduction

The ultimate goal of the Large Hardon Collider (LHC) is to discover new physics. With the advent of colliders of extremely high energies such as the LHC, much of the knowledge in physics is being pushed to the frontier, where our understanding of physics becomes less and less. Therefore, the goal to find new physics is motivated by our wish to explain all that is not understood in this new frontier of high energy.

A method for searching for new physics involves testing specific theories of new physics by comparing experimental data with theoretical predictions. These specific theories can be split into two categories: all-encompassing theories which attempt to give deep explanations of phenomena – the Standard Model being one – and "effective" theories which build upon what we already have. One effective theory considers the possibility of composite quarks, which are viewed as bound states of more fundamental particles called preons. This idea is naturally drawn from previous experiences in physics: from indivisible atoms, to atoms being bound states of electrons and nucleons (protons, neutrons), to those nucleons being composed of more fundamental particles called quarks and gluons. The compositeness of quarks suggest the possibility for new strong forces whose details manifest themselves at energies beyond that currently available at the LHC.

To test this theory, consider the measurements made by the CMS group of proton-proton collisions. More explicitly, we study the reaction

$$p + p \to j + X, \tag{1}$$

where j is a spray of particles called a jet and X could be anything else. The magnitude of the transverse momentum, denoted $p_T = |\overrightarrow{p_T}|$, of every jet is measured along with the polar angle θ, which is the angle with respect to the trajectory of the proton beam line – that is, the z-axis. What is usually measured is the pseudorapidity η, defined as $\eta = -\ln\tan(\frac{\theta}{2})$. All jets with $|\eta| < 0.5$ have their p_T binned into a histogram, which gives a falling spectrum referred to as the inclusive jet transverse momentum spectrum. It is this spectrum that previously mentioned effective theory makes predictions for.

Because an effective theory builds upon what we already know, we must first discuss briefly the quantum field theory called the Standard Model. But, what is a quantum field theory (QFT)? A field is a quantity whose elements are presumed to exist at every point in space-time. A quantum field is then a field whose elements also obey the rules of quantum mechanics. The theory describes each particle through an appropriate quantum field. Mathematically, the details of a QFT are contained in a function called the Lagrangian L, which is related to the action S by the equation

$$S = \int d^4x L(\psi, ...), \tag{2}$$

where the integral is over 4 dimensions – three spatial and one temporal – and ψ being one quantum field of many. We know from quantum mechanics that the momentum p can be expressed as

$$p = \frac{h}{\lambda}, \tag{3}$$

where h is Planck's constant and λ is a characteristic length associated with a particle. If we take units such that $\hbar \equiv \frac{h}{2\pi} = 1$ and the speed of light (in vacuum) $c = 1$, we can check that the units of the characteristic length is given by

$$\lambda = \frac{h}{p} \rightarrow \lambda = \frac{1}{p} = \frac{1}{mc} \rightarrow \lambda = \frac{1}{m}.$$

So we see that distance has units of $mass^{-1} \equiv M^{-1}$. It follows then that because the action S is dimensionless and that d^4x has units of M^{-4}, then the Lagrangian L must have dimensions of M^4. The current view of the Standard Model is that it itself is an effective theory that is part of a "complete" theory described by the Lagrangian

$$L_{complete} \approx L_{SM} + \frac{1}{\Lambda} L_5 + \frac{1}{\Lambda^2} L_6 + ..., \tag{4}$$

where L_{SM} is the Standard Model Lagrangian, L_5 is a term of dimensionality M^5 (dim-5), L_6 is a term of dimensionality M^6 (dim-6), etc, and Λ is a scale factor called the mass scale that is introduced to get the correct dimensions. We are particularly interested in the L_6 term, which describes a four-fermion interaction at a point called a contact interaction (CI). Because the mass of the theorized mediator between the quark interactions is much larger than the energy scale at which the interactions occur, they can be modelled by contact interactions determined by the mass scale Λ. Such a model is similar to Enrico Fermi's explanation of the β-decay of a neutron, for which the coupling occurs at a single vertex (Figure 1). Contact interactions are thus of the same form as Fermi's interaction, an interaction between particles at a single vertex. This model provides a way to analyze interactions without the need to understand the details of the interaction.

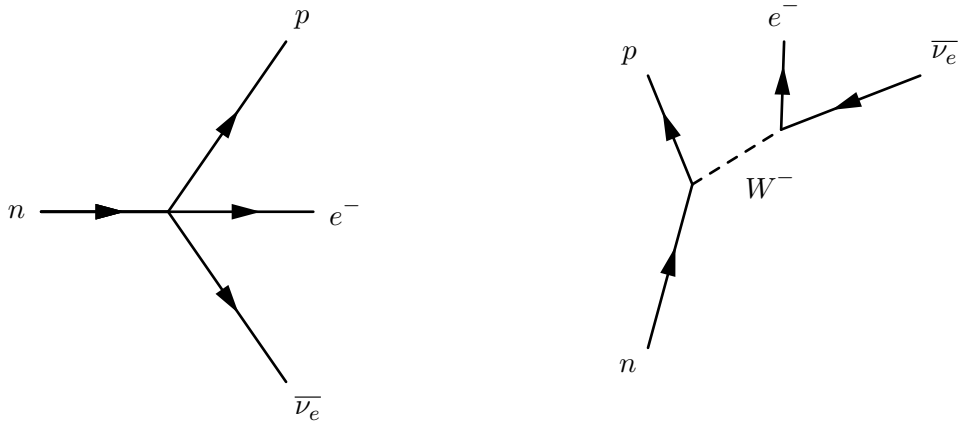

Fig. 1: Left side: Fermi interaction of β-decay. Right side: Exchange interaction of β-decay

Of course, one would prefer to be able to model interactions in the more modern manner of exchange interactions (Figure 1, right side). Yet, as previously mentioned, the mass of the exchange particle is so heavy that its interaction cannot be resolved at the LHC. We are thus inclined to approximate potential preon interactions as contact interactions.

In this work, we will search for any discrepancy between the CI model and the Standard Model. If no significant discrepancy is found, a lower limit will be set for the mass scale Λ that will determine a range for the possibility of new physics.

2 Project Description

The goal of this study is to find any deviation between the CI jet spectrum and the quantum chromodynamics (QCD) jet spectrum as predicted by the Standard Model. Failing to find any deviation, we will be made to calculate a lower limit for the mass scale Λ for the CI model. The effective Lagrangian of the CI model is defined by [cite paper in CI],

$$L_{CI} = 2\pi\lambda \sum_{i=1}^{6} \kappa_i O_i, \tag{5}$$

where $\lambda = 1/\Lambda^2$, κ_i are constants that denote constructive or destructive interference ($\kappa = -1$ and $\kappa = +1$, respectively), and O_i are 6 dimensional operators that describe a four-quark interaction ($\overline{\psi}\psi\overline{\psi}\psi$, where each ψ is dim-3/2). If this Lagrangian term were to exist as part of the complete Lagrangian, a consequence would be that we would see an increase in the scattering cross section of the jet as the p_T increases. One explanation for this behaviour would be that the four interacting fermions – in this case quarks – are made of constituent particles that would provide for more scattering centers and therefore a higher cross section.

2.1 Inclusive Jet Spectrum Cross Section

To study this CI model, we will need to generate and analyze, to next-leading-order, the inclusive jet p_T spectrum cross section given by,

$$\sigma = \sigma_{QCD} + \sigma_{CI}, \tag{6}$$

where σ_{QCD} is the cross section given by QCD and σ_{CI} is the cross section given by CI, which depends on κ_i, λ, and coefficients a and b, defined below.

Symbolically, the cross section is given by

$$f(p_T) \equiv \sigma = \sum_{i,j} \int_0^1 dx_1 \int_0^1 dx_2 f_i(x_1, \mu_F) f_j(x_2, \mu_F) \hat{\sigma}(x_1, x_2, p_T, \mu_F, \mu_R) \tag{7}$$

where x_1 and x_2 are momentum fractions, $f_i(x_1)$ and $f_j(x_2)$ are parton distribution functions (PDF), μ_F is the factorization scale, μ_R is the renormalization scale, and $\hat{\sigma}$ is the parton-level cross-section. The summation over i and j indicates the sum over all possible partons in the two interacting protons. The PDF's describe the probabilities that partons with certain momentum fractions will collide. In this study, we used the PDF's provided by CT10 [cite CTEQ].

The parton-level cross section $\hat{\sigma}$ is a function of $|M|^2$, where M is the complex matrix element that describes the four-fermion interaction. The matrix element M can be expressed as,

$$M = M_{QCD} + \frac{1}{\Lambda^2} M_{CI}, \tag{8}$$

where M_{QCD} is the matrix element described by QCD and M_{CI} is the matrix element described by the four-fermion contact interaction. The absolute square of M is then

$$|M|^2 = |M_{QCD}|^2 + \frac{1}{\Lambda^2}(M^*_{QCD} M_{CI} + M^*_{CI} M_{QCD}) + \frac{1}{\Lambda^4}|M_{CI}|^2. \tag{9}$$

In order to calculate the quantity $|M|^2$, we use the FastNLO program [cite FastNLO location] for calculating the $|M_{QCD}|^2$ term and the CIJET program [cite CIJET location] to get the Λ-dependent terms.

2.2 Uncertainties

One problem with using PDF's is that they contain parameters that are uncertain. To account for these uncertainties in our calculations, a set of 500 PDF's were randomly generated by varying the parameters of the PDF's. This yields a set of cross sections for each p_T bin. What must also be taken into consideration is the uncertainty produced by the CMS detector itself. To do this we "smear" the QCD spectra, $f(p_T)$, using the jet response function $R(p_{T,obs}, p_{T,true})$, where $p_{T,obs}$ denotes the observed jet transverse momentum and $p_{T,true}$ is the true jet transverse momentum. This smearing can be represented as a convolution of the spectra with the response function,

$$f_{obs}(p_{T,obs}) = \int R(p_{T,obs}, p_{T,true}) f(p_T) dp_T. \tag{10}$$

This convolution produces what is referred to as the smeared QCD p_T spectrum.

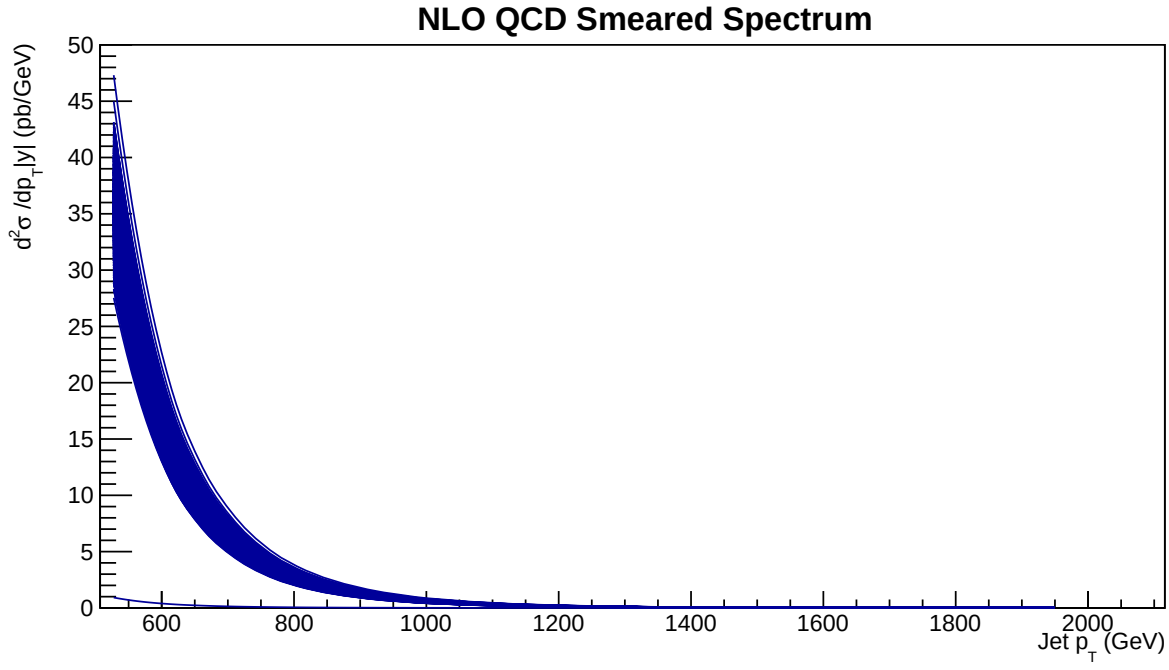

Fig. 2: Falling smeared QCD spectrum.

The CI spectrum requires more work than the QCD spectrum in that we must calculate the appropriate coefficients for σ_{CI} and check that the spectrum behaves smoothly, as well as smearing the CI spectrum. The full CI term in the inclusive jet p_T cross section per bin can be written as [cite CI paper]

$$\begin{aligned}
\sigma_{CI} = \lambda \sum_{i=1}^{6} \kappa_i (b_i + a_i g + a_i f) \\
+ \lambda^2 \sum_{i=1}^{6} \kappa_i^2 (b_{ii} + a_{ii} g + a_{ii} f) \\
+ \lambda^2 \sum_{i=1,3,5} \kappa_i \kappa_{i+1} (b_{ii+1} + a_{ii+1} g + a_{ii+1} f) \\
+ \lambda^2 \sum_{i=1,2,5,6} \kappa_i \kappa_4 (b_{i4} + a_{i4} g + a_{i4} f)
\end{aligned} \tag{11}$$

where $g = -\ln(\mu_0 \sqrt{k})$, $f = \ln(\sqrt{\frac{k}{\lambda}})$, μ_0 is an arbitrary scale provided by the CIJET program, and k is another arbitrary scale that we are free to choose. The CIJET program was used to calculate each of the a_i, a_{ii}, b_i, and b_{ii} coefficients.

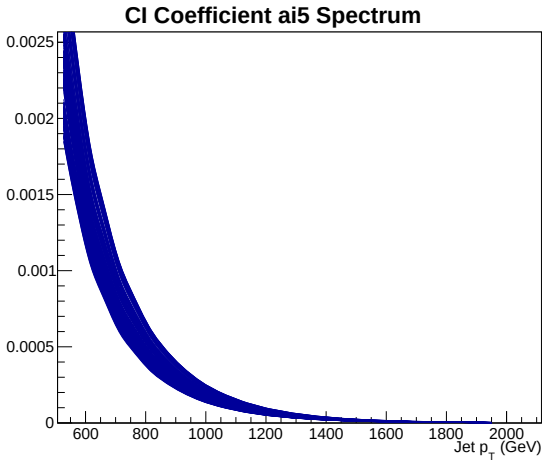

Fig. 3: Smeared coefficient for CI term.

We can see from Figure.3 that one of the coefficients exhibits smooth behaviour. A was written to check each of these CI coefficients, all of which behaved smoothly. This procedure of checking each coefficient, while tedious, is necessary to ensure that future computations that utilize the CI spectrum will not behave oddly – or rather any odd behaviour will not be a result of poorly constructed coefficients. Using these smeared coefficients, a spectrum for the CI term can now be computed and used for the total cross section.

The next thing to do is to check the behaviour of the total cross section, Eq.(6), and the QCD cross section. To do this, the ratio $\sigma_{total}/\sigma_{QCD}$ was graphed for different Λ values.

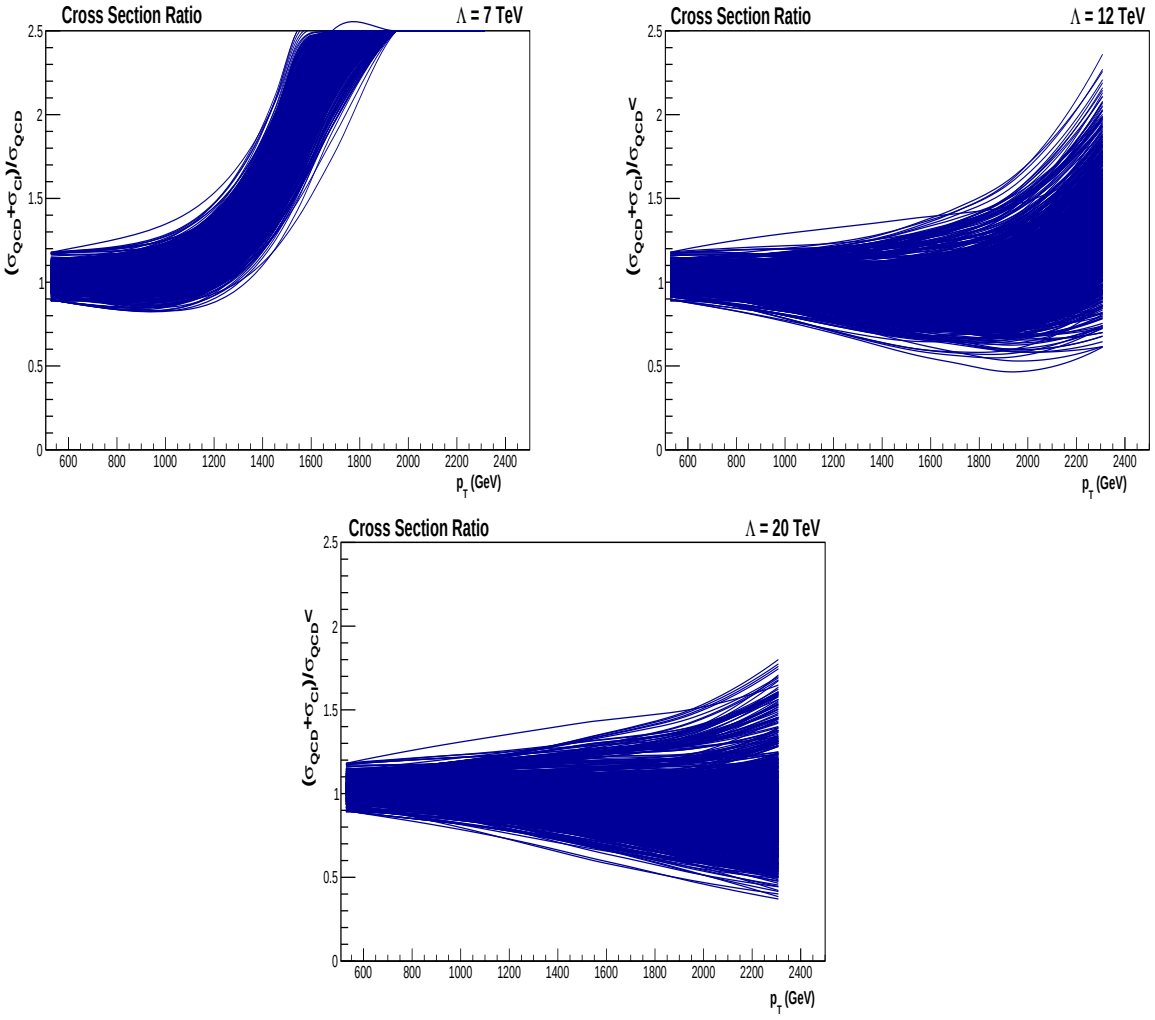

Fig. 4: Histograms displaying the ratios for the total spectrum over the QCD spectrum for Λ values of 7, 12, and 20 TeV. For these histograms, $\kappa_1 = +1$ and the rest $\kappa_i = 0$, corresponding to the LL-model. Note how the ratios become closer to 1 as Λ increases.

Similar histograms were made using $\kappa_1 = -1$ and $\kappa_{i\neq 1} = 0$, also corresponding to the LL-model,

with identical behaviours with the exception of lower Λ values. The next thing that was done was to check the CI spectrum in the same manner as done with the QCD spectrum.

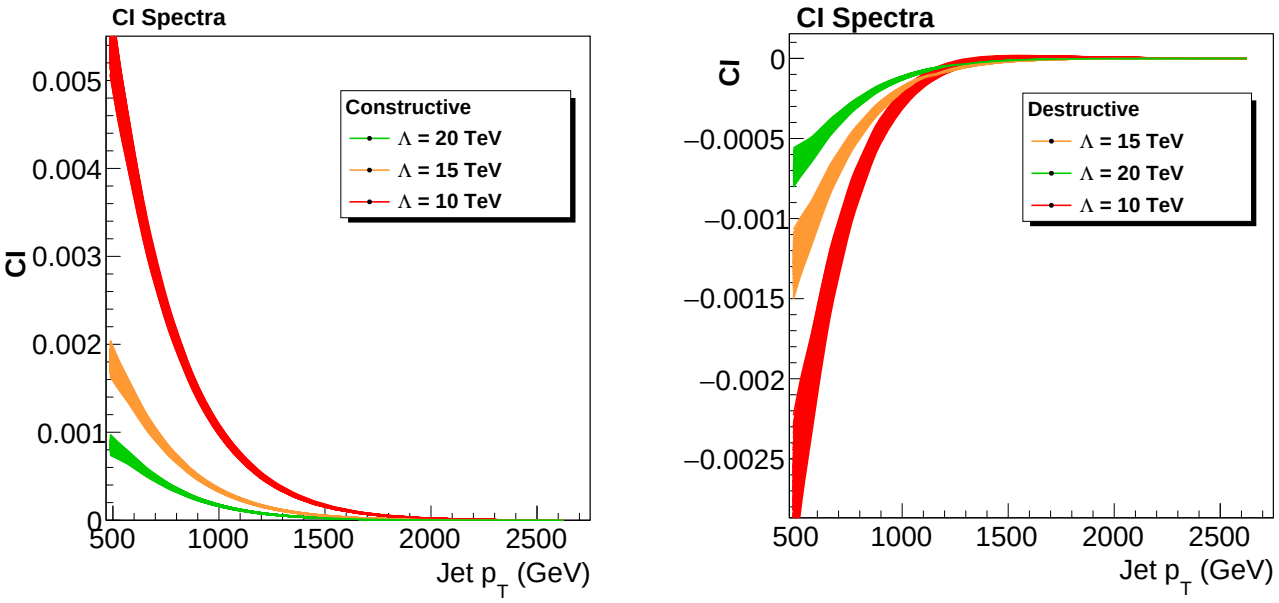

Fig. 5: Left: Constructive CI spectrum. Right: Destructive CI spectrum. Spectra taken over different Λ values to show the magnitude of contribution to the overall cross section.

Figure.5 shows the smooth behaviour of the CI spectra for different Λ values. It should be noted that the spectra approach 0 as the p_T increases. The contribution from the CI spectra appear to contribute very little to the total cross section at higher energies.

2.3 Likelihoods

If no discrepancy is found between the data and the QCD prediction, we shall set an upper limit on λ as follows. We denote by $p(\lambda|N)$ the probability of getting λ given N, where $N = N_1, ..., N_i$ are the jet counts per p_T bin. Using Baye's Theorem, we can rewrite $p(\lambda|N)$ as,

$$p(\lambda|N) = \frac{p(N|\lambda)p(\lambda)}{p(N)} \tag{12}$$

For simplicity we assume that $p(\lambda) = 1$. The term $p(N|\lambda)$ is the multinomial likelihood, which can be expressed as

$$p(N|\lambda) = \int \left(\prod_{i=1}^{M} \left(\frac{\sigma_i(\lambda, \omega)}{\sigma_{tot}} \right)^{N_i} \right) d\omega, \tag{13}$$

where $\sigma_i(\lambda, \omega)$ is the cross section (as defined by Eq. (6)) in bin i of the jet p_T, $\sigma_{tot} \equiv \sum_{j=1}^{M} \sigma_i$ is the total cross section taken across all histogram bins, N_i is the count in bin i of the jet p_T, M is the number of bins (16 in our study), and ω denotes the nuisance parameters such as the PDF variables, the parameters μ_F and μ_R, the jet energy scale (JES), and the jet energy resolution (JER). To account for the uncertainties we integrate over ω.

To make sure we have a good enough sample size to take uncertainty into consideration, 10,000 cross section spectra were made, varying all the parameters that contain uncertainties. The average was

then taken

$$p(N|\lambda) \approx \frac{1}{K}\sum_{k=1}^{K}\prod_{i=1}^{M}\left[\frac{\sigma_i(\lambda,\omega_k)}{\sigma_{tot}}\right]^{N_i}, \tag{14}$$

where $K = 10,000$.

A limit on λ with a confidence level of 95% is found by solving

$$\int_0^{\lambda_{up}} p(\lambda|N)d\lambda = 0.95. \tag{15}$$

This tells us that there is a 95% probability that λ lies within the range $0 < \lambda < \lambda_{up}$, where λ_{up} is the upper limit. From this, the mass scale Λ can be extracted.

3 Results

3.1 Discrepancy Between CMS Data and the CI Model

The relation of the $\sqrt{s} = 8$ TeV data from CMS to the predictions made by the CI model are displayed below:

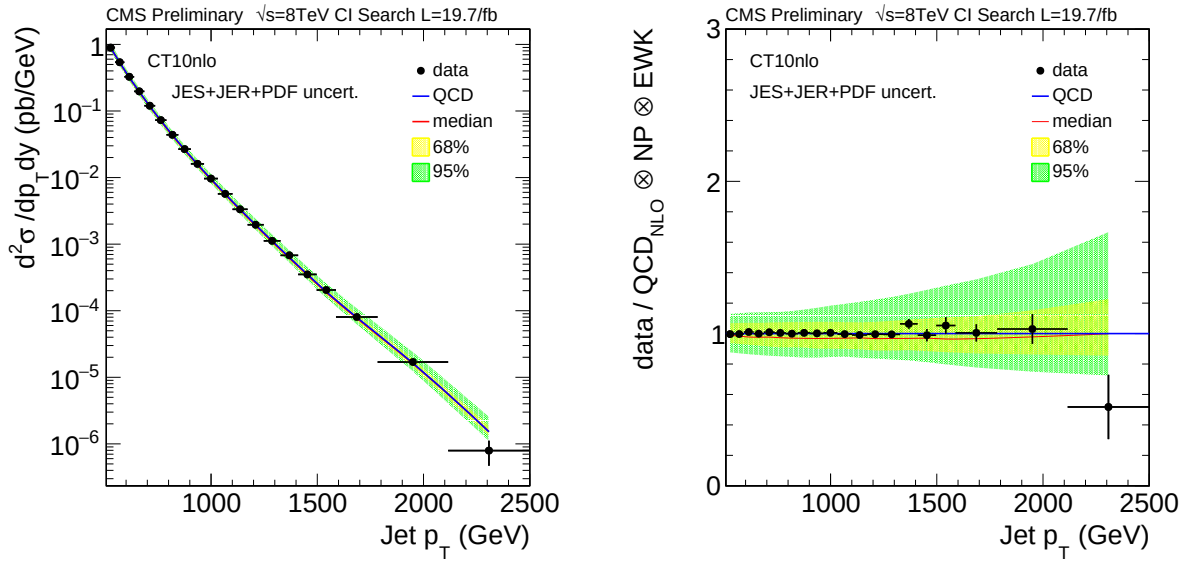

Fig. 6: Left: Graph of the cross section provided by the $\sqrt{s} = 8$ TeV data along side QCD prediction. Right: Graph of the ratio of the data with the QCD+uncertainties. The blue line indicates the QCD prediction. The colored bands refer to the uncertainties from jet energy spectrum (JES), jet energy response (JER), and the parton distribution functions (PDF).

From Figure.6, we see that the data matches the QCD prediction with great accuracy along not only the cross section spectrum but along the ratio as well. This indicates that there is no apparent deviation between the data and the QCD prediction. Therefore, a lower limit for the CI mass scale Λ for the left-left contact interaction model described by Eq.(5) will be computed. Two particular Λ values were determined: one for $\kappa_1 = +1$ and one for $\kappa_1 = -1$, which correspond to destructive and constructive interference, respectively.

3.2 Lower Limit On the Mass Scale Λ

To get an idea of the relation between the data and Λ, histograms like the those in Figure.6 were graphed for both constructive and destructive interferences.

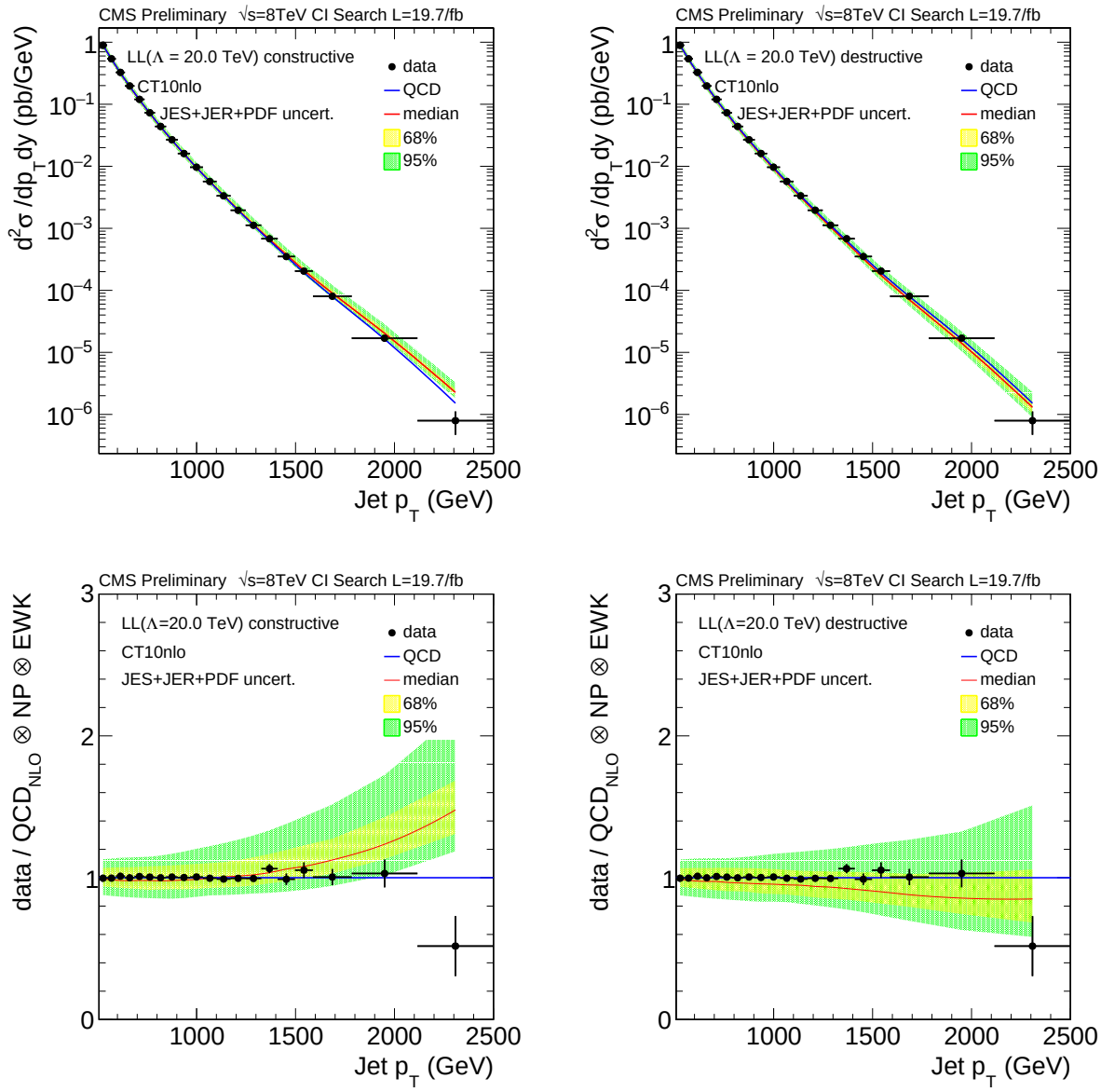

Fig. 7: Histograms of the LL model for $\kappa_1 = -1$ (left side) and $\kappa_1 = +1$ (right side) graphed in relation to the CMS data. The colored bands indicate the uncertainties from JER, JES, and PDF. $\Lambda = 20$ TeV for these histograms.

The data closely matches the LL model up until $\sim$1500 TeV. After this point, the data starts deviating from the CI model. From the likelihood calculations, we acquire the graphs in Figure.8. Due to the uncertainties that propagate all the way through to the likelihood calculations, each generation of Λ is never exactly the same but within the same order of magnitude. The results gathered by Figure.8 tell us that the lower limits are $\Lambda = 22.7$ TeV (constructive) and $\Lambda = 13.9$ TeV (destructive) with 95% confidence level.

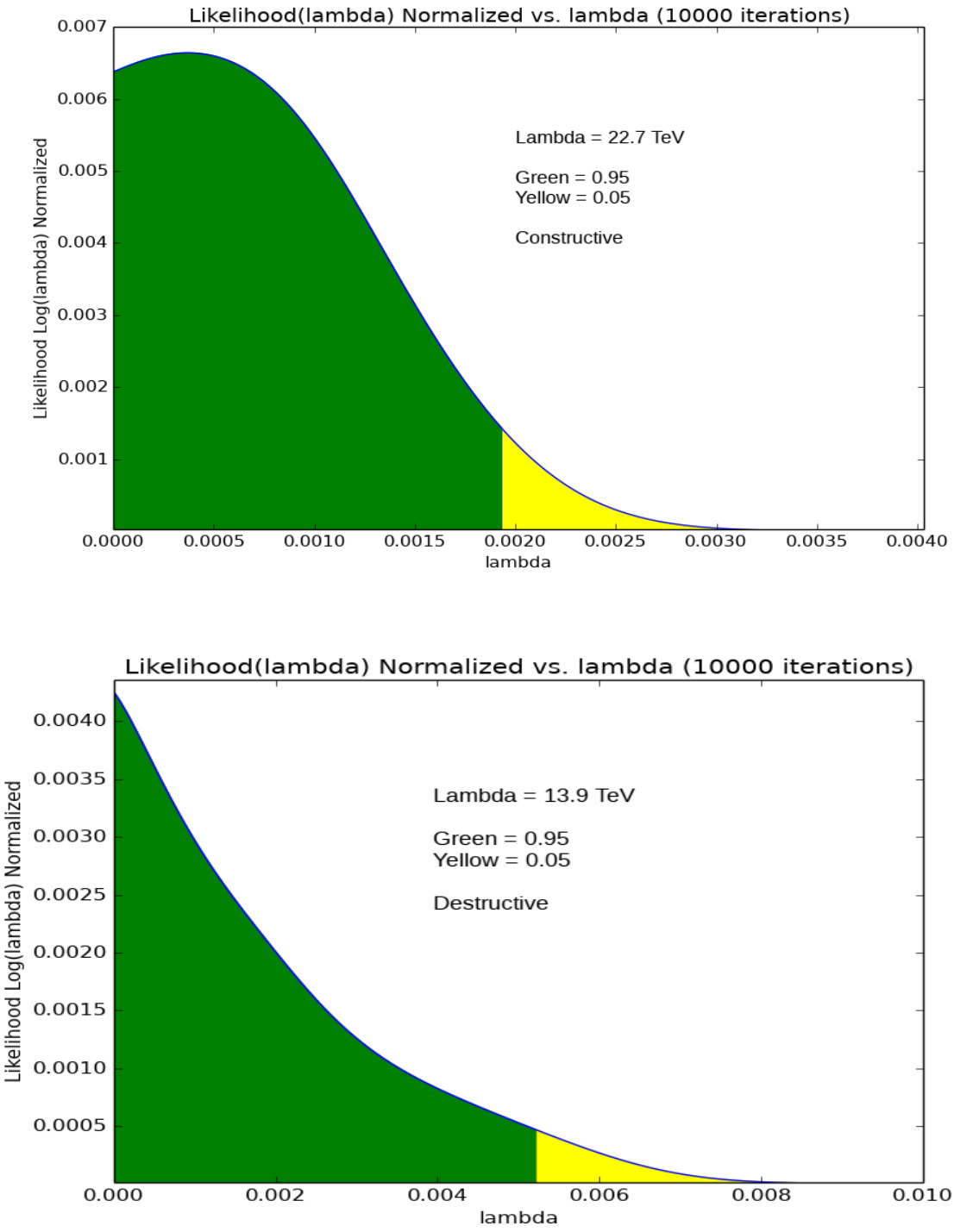

Fig. 8: Top: Normalized likelihood plot for Λ when $\kappa_1 = -1$, indicating constructive interference. The green portion represents where 95% of the λ values fall and the yellow portion represents where the remaining 0.05% lie. The horizontal axis shows the range of $\lambda = 1/\Lambda^2$ values; a smaller λ value will translate to a larger Λ. The vertical axis gives the likelihood of λ as a logarithm. The likelihood was calculated using 10,000 randomly sampled spectra of both QCD and CI. Bottom: Similar plot but with $\kappa_1 = +1$. Here we see that Λ is smaller for destructive interference than it is for constructive. 10,000 randomly sampled spectra for QCD and CI were also used to construct this.

References

eserved for citations.